

Applied Ion Systems

AIS-TR-012

AIS-ILIS1 Ionic Liquid Ion Source Electropray Thruster V6

Fueling and Ignition Test 3 - 08/16/2020

Testing Report and Summary

Michael Bretti – 08/30/2020

I. TEST PARAMETERS

- **System:** AIS-ILIS1 Ionic Liquid Ion Source Electro spray Thruster V6
- **Fuel:** EMI-BF4
- **Maximum Chamber Pressure During Testing:** 2×10^{-5} Torr
- **Testing Status:** COMPLETE
 - **Phase I:** Fueling – SUCCESS
 - **Phase II:** Ignition – UNSUCCESSFUL

II. OVERVIEW

This test is the third fueling and ignition test of the AIS-ILIS1 ionic liquid ion source electro spray thruster for nanosatellites. This thruster is one of many open-source, ultra-low cost, advanced electric propulsion systems in development at AIS, and is currently the most advanced thruster build at AIS to date.

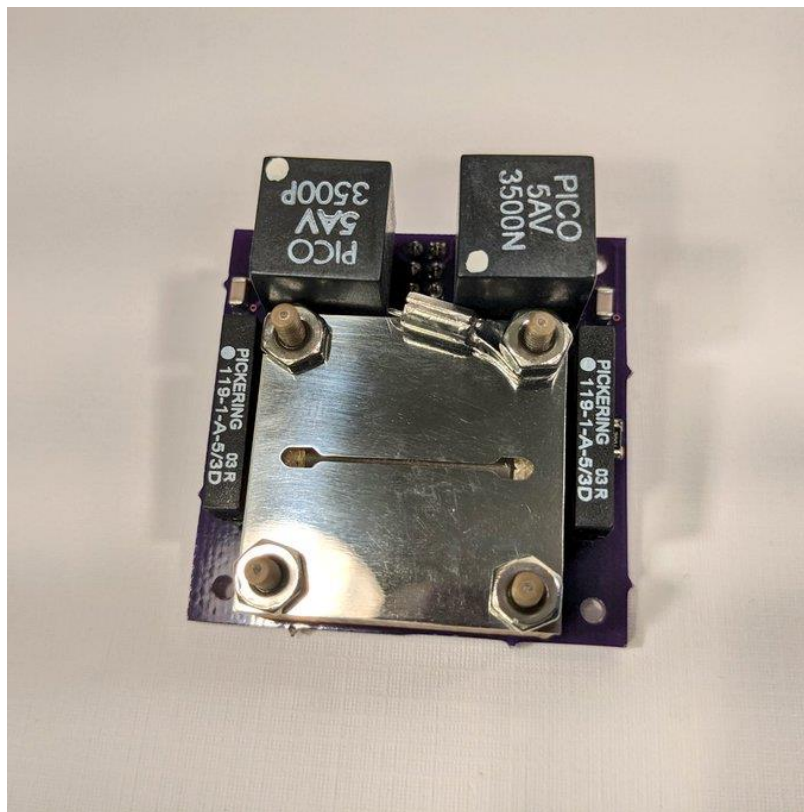


FIGURE 1: Completed AIS-ILIS1 V6 thruster assembly

The AIS-ILIS1 aims to solve issues of ion thruster scaling and accessibility for nanosatellites, at significant cost reduction to currently available micro-ion thrusters on the market, as well as being the first ever PocketQube class compatible ion thruster, in size, power requirements, and

fueling restrictions. The ILIS1 represents a new and fundamental shift in micro-ion thruster technology development, allowing for performance ion thrusters to be available for any nanosatellite team, serving a wide range of uses from main propulsion for station keeping, orbital transfers, collision avoidance, formation flying, and deorbiting, to secondary propulsion for fine attitude control.

The following report details the fueling and ignition tests of the ILIS1 using the new V6 thruster board, as well as analysis, results, and conclusions moving forward for future testing and system improvements.

III. PRELIMINARY THRUSTER MOIFICATIONS

During prior testing of the ILIS1, it was found that emission would concentrate at the corners or the ridge emitter, rather than along the length of the ridge itself. Due to the sharp edge, higher field enhancement results at the corner, causing early turn-on, as well as excessive emission concentration at this area. In order to reduce field enhancement at the corners, and achieve more uniform field distribution along the length of the ridge, a modified, enhanced extractor geometry was developed. Instead of a linear slit which is traditional for ridge or slit based electro spray, the last several mm at each end was flared out significantly, in addition to the central region of the slit being reduced further in width.

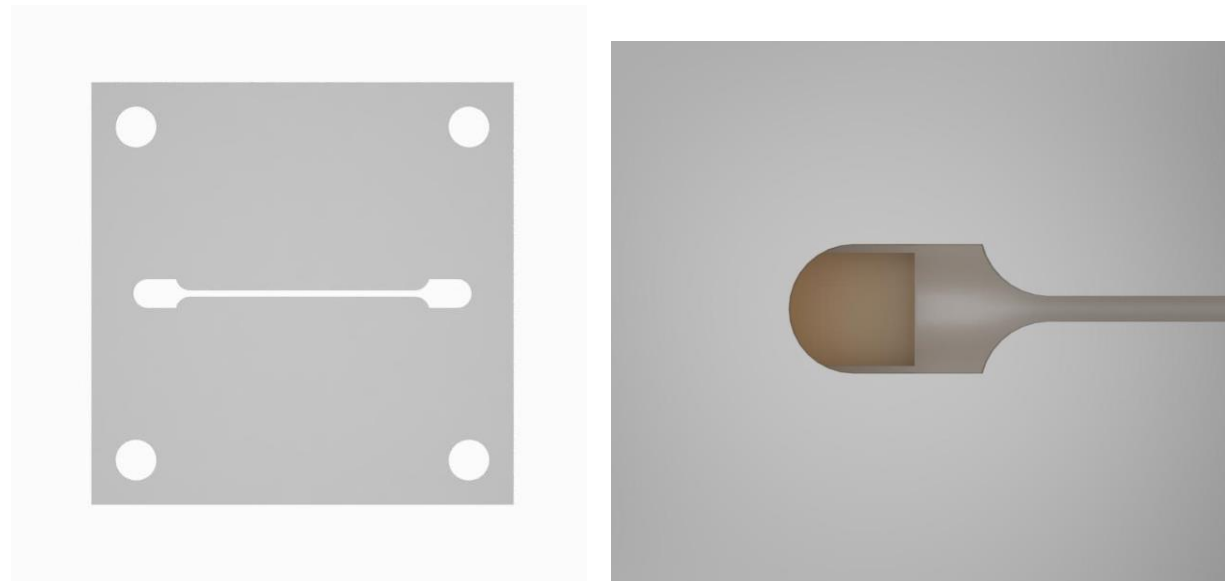


FIGURE 2 & 3: Enhanced extractor design with flared edges (LEFT), flare geometry and emitter alignment close-up (RIGHT)

Electrostatic field simulation results show that field enhancement is significantly reduced at the corner, with the main portion of the ridge having much higher field strength. Although there is some higher field strength at the edge still, it remains lower than the central region at all times, eliminating early turn-on at the edges and forcing emission to occur across the bulk of the slit.

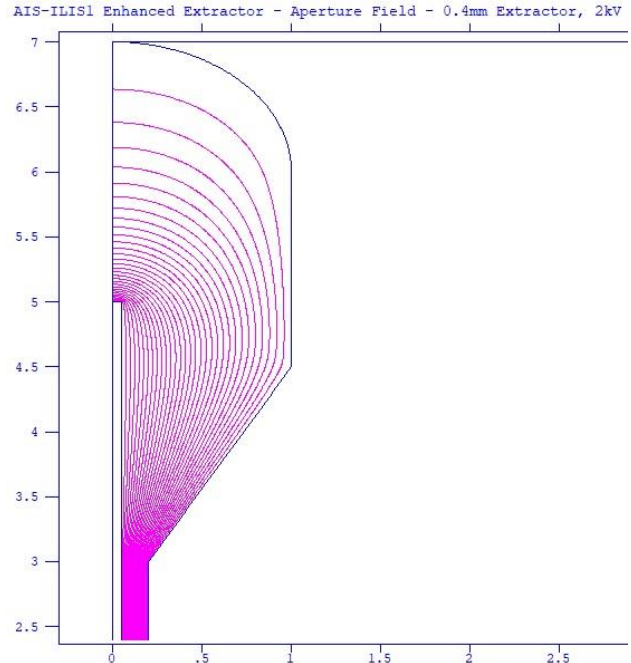
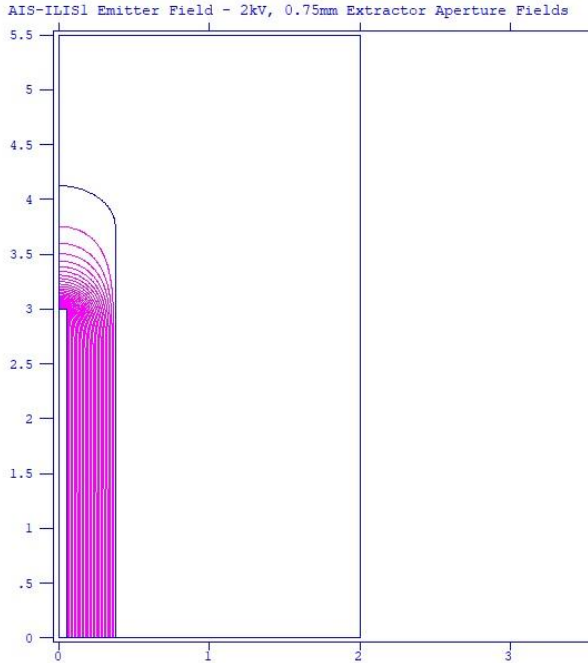


FIGURE 4 & 5: Prior extractor design field strength (LEFT), enhanced extractor design field strength (RIGHT)

In addition, a slightly thicker extractor plate was used, at 250um vs the original 100um. Field simulations show reduced field divergence as a result, which translates to reduced beam divergence. The thinner slit aperture also serves to further increased field strength at the ridge emitter, with the aim to cause emission to start at lower voltages.

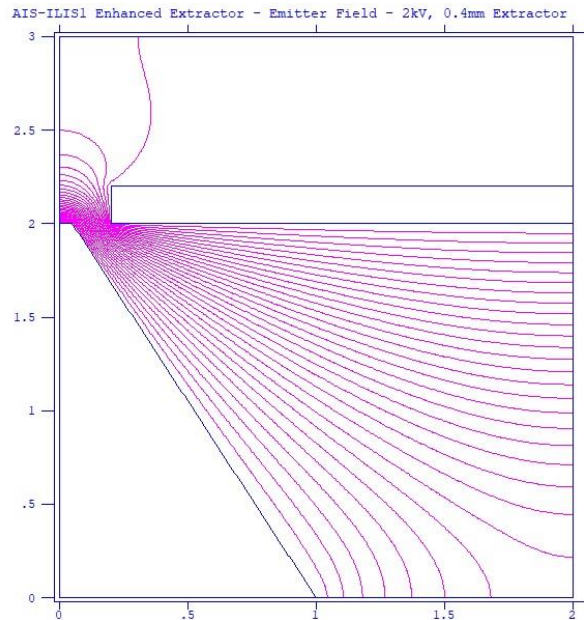
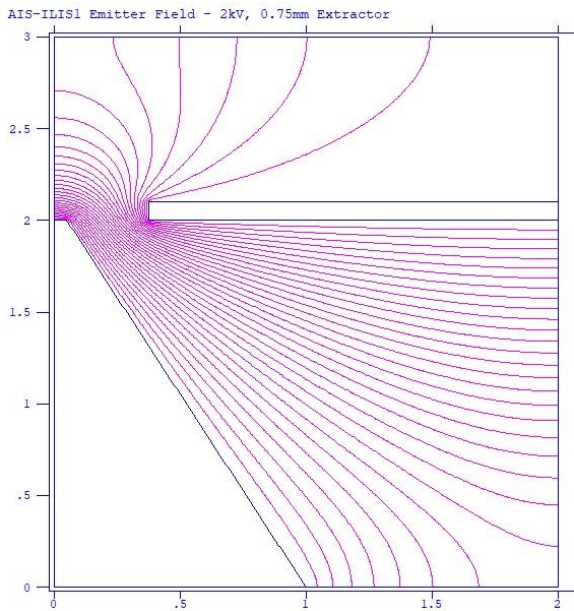


FIGURE 6 & 7: Prior extractor design field strength cross-sectional view (LEFT), enhanced extractor design field strength cross-sectional view (RIGHT)

The final extractors were fabricated from 250um spring-temper stainless steel sheet. Three sets of both 400um and 500um width apertures were made.

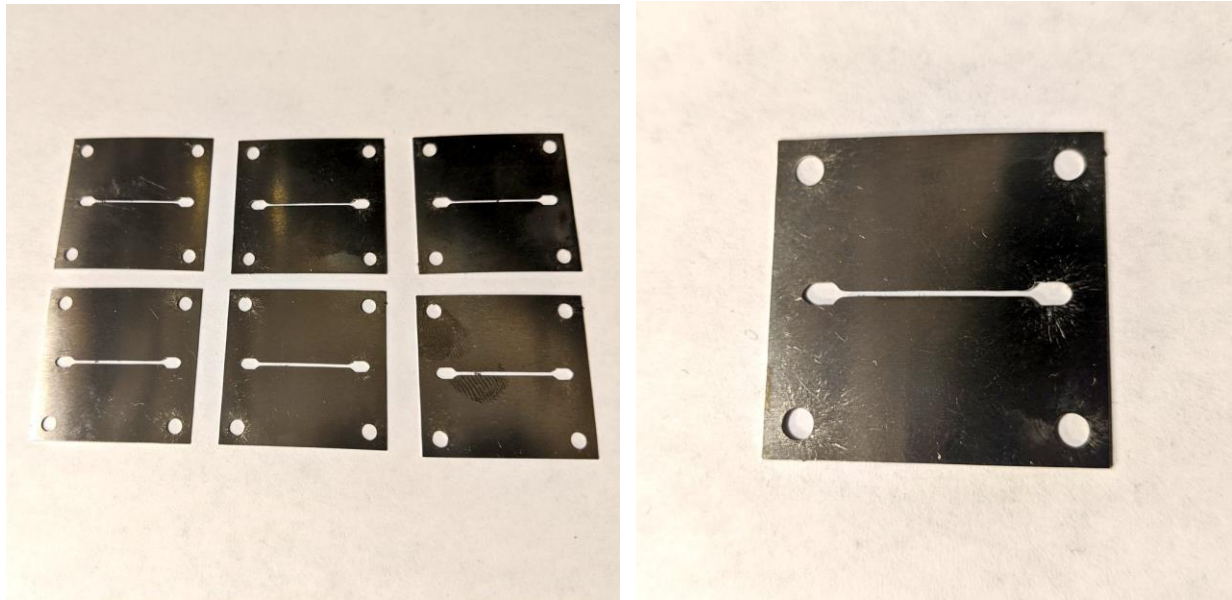


FIGURE 8 & 9: Enhanced extractor sets, 0.4mm top, 0.5mm bottom (LEFT), enhanced extractor (RIGHT)

Upon arrival and inspection of the new extractors, it was discovered that the laser cut edges were of extremely poor quality, exhibiting significant dross, unevenness, burrs, and charring. The edges were manually cleaned and polished using 3000 grit sandpaper, and both faces of the extractor were polished with 3000 grit sandpaper as well.

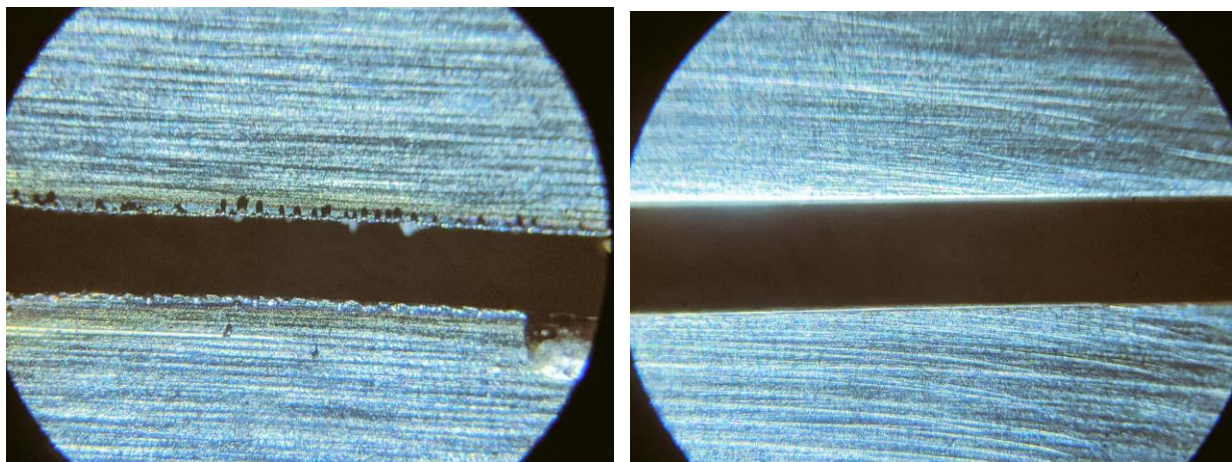


FIGURE 10 & 11: Microscope view of extractor slit upon arrival (LEFT), extractor slit post-processing (RIGHT)

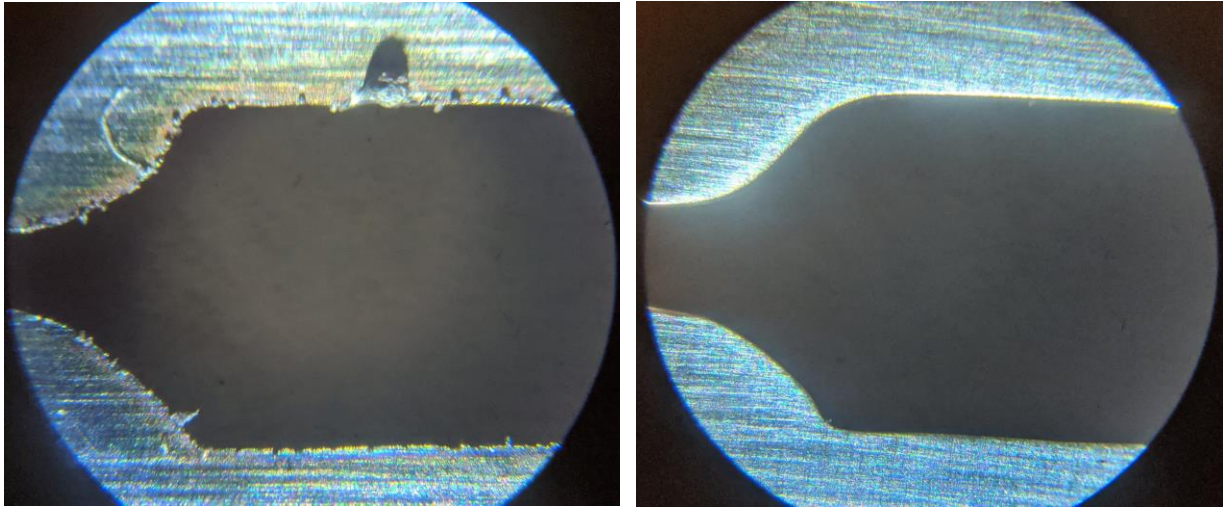


FIGURE 12 & 13: *Microscope view of extractor slit end flare upon arrival (LEFT), extractor slit end flare post-processing (RIGHT)*

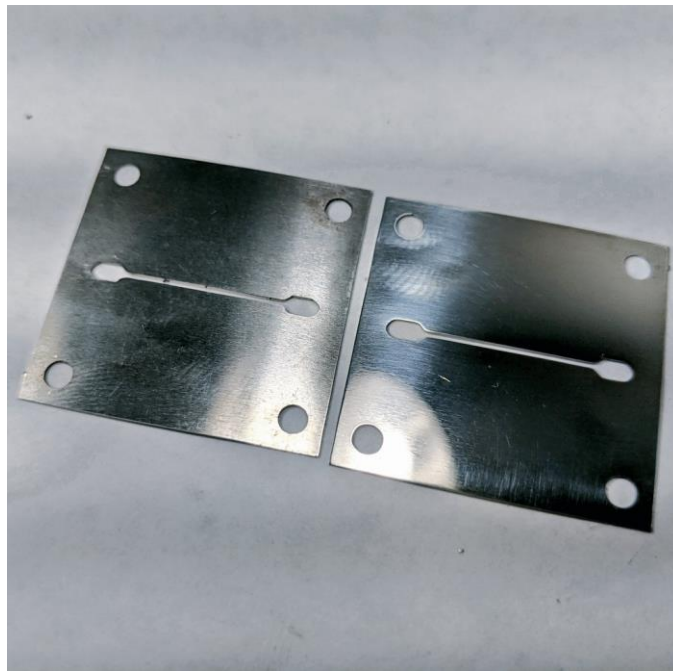


FIGURE 14: *Comparison of original (left) and polished (right) extractors*

During the prior test, the thruster eventually shorted due to charring of the fuel caused by liquid creep along the 3D printed Ultem 1010 housing between the emitter and extractor. As a result, the 3D printed thruster housing design was modified to minimize plastic around the ridge to prevent direct liquid creep along the surface, which would cause shorting over time. Small tabs were created on the very ends of the ridge emitter for positioning and alignment of the ridge.

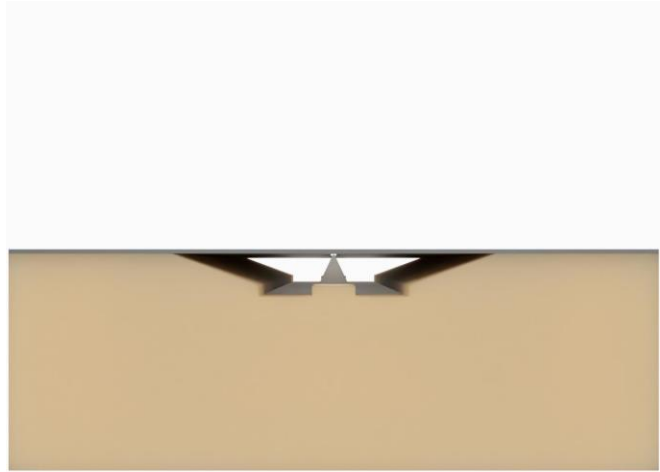


FIGURE 15 & 16: Concept design of the enhanced thruster housing with emitter (LEFT), side view of thruster housing with emitter and extractor alignment (RIGHT)

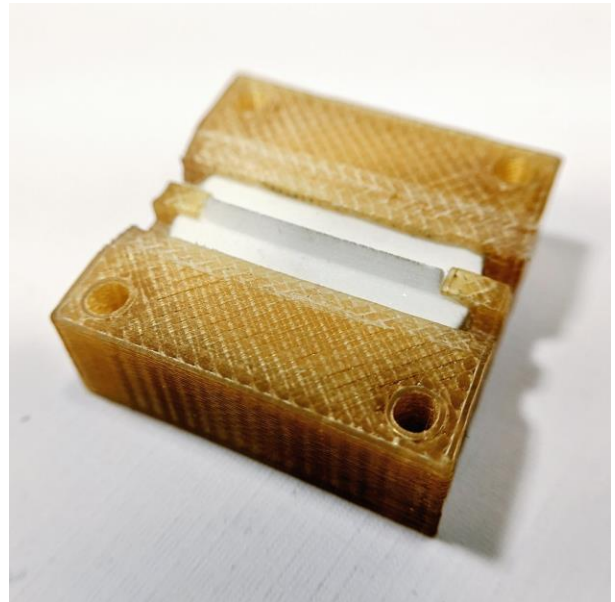
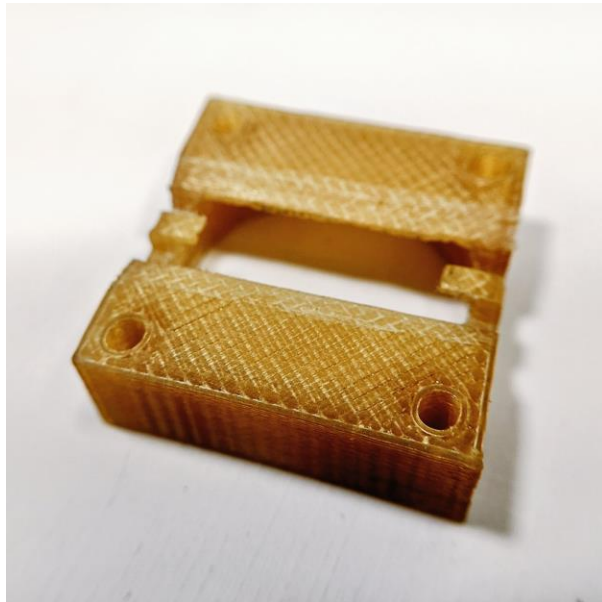


FIGURE 17 & 18: Modified 3D printed Ultem 1010 housing (LEFT), housing with emitter for test fit and alignment (RIGHT)

In addition, previous testing suggested the thruster had been operating in mixed mode operation, with both droplet and ion beam emission, evident due to the buildup of some ionic liquid on the back face of the extractor plate. Colloidal, mixed mode, or purely ionic emission is governed by emitter properties and design, fuel flow rate, and extractor potential. In order to better achieve purely ionic emission and reduce droplet emission, the reservoir was changed from P2 grade

porous frit to P3 grade porous frit, which would significantly reduce capillary flow rates by reducing capillary pressure applied from the reservoir to the emitter.

Finally, the thruster circuit boards were modified to include additional surge protection resistors to limit arcing current, and subsequent thruster damage due to breakdowns during operation. 100k resistors were placed between the output of the HV isolation relays and the emitter contact pad, and between the HV filter capacitor and the emitter contact pad. In addition, a 100k resistor was placed between the extractor plate and ground, further reducing surge currents, as well as allowing for beam intercept current on the extractor for future tests. Due to these changes, the high voltage divider readout was slightly modified to compensate for these changes to provide accurate readings, which was tested against the ILIS1 HV test load.

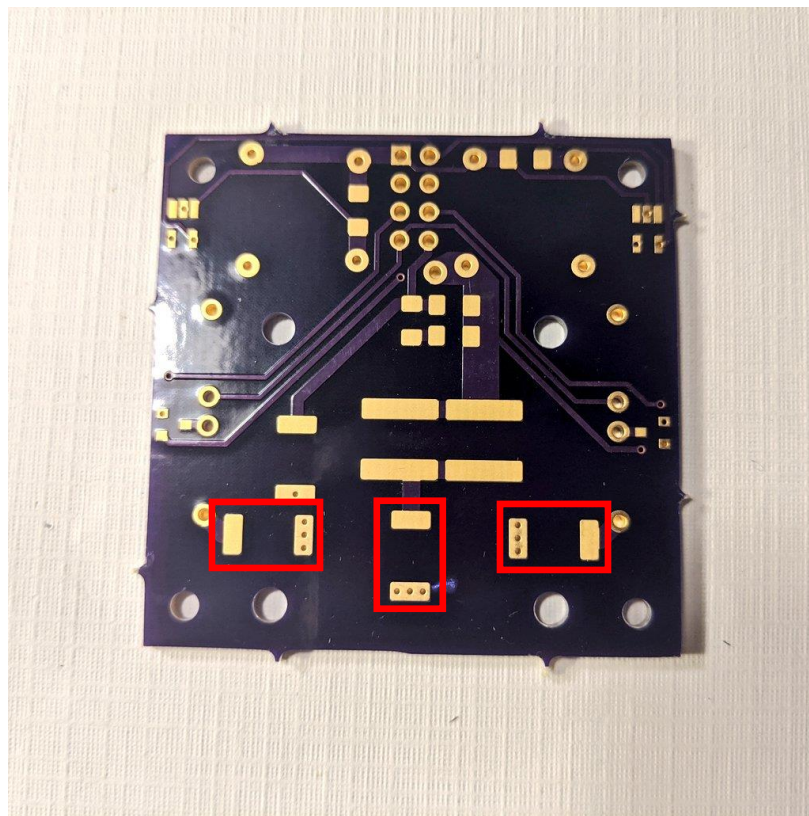


FIGURE 19: New V6 PCB design with 100k HV SMT surge protection resistors (outlined in red boxes)

IV. TEST PHASE I – FUELING AND BAKEOUT

The fueling and baking procedure for the ionic liquid fuel and Ultem 1010 housing remained the same as the prior test. Both the porous glass emitter and reservoir were placed in their own separate Pyrex beaker, just large enough to fit the 25mm diameter discs. The beakers were then

filled with ionic liquid just barely over each of the discs. The rest of each beaker was filled with 316 stainless steel wool at the top to act as a baffle to prevent excessive splattering as well as keeping the discs from bouncing around. The tops of the beakers were then covered tightly with aluminum foil to further prevent any droplet spray into the chamber during pump-down and degassing.

The filled beakers, Ultem printed housing, and vacuum thermocouple, were mounted on a scrap PEEK baseplate that rested inside the chamber, to prevent direct heating from the chamber during bakeout. The system was pre-pumped with the roughing pump the night prior and sealed to facilitate faster pumpdown during the fueling phase of the test.



FIGURE 20: Saturated porous glass emitter and reservoir with Ultem housing on PEEK baseplate for baking and degassing

The internal temperature was maintained between 65-80C for a duration of 2.5 hours, at which the chamber was kept at a vacuum level of around 2×10^{-5} Torr. After the baking and degassing cycle was complete, and the system shut down and allowed to cool, preparations were made for the second phase of the test.

V. IGNITION TEST SETUP

After fueling was completed, final assembly and system preparations were made for the next phase of ignition testing. The thruster components were cleaned, and with the fully loaded emitter and reservoir, assembled into the final thruster. The thruster was then mounted to the Faraday cup test stand, which is used to collect and measure beam current, verifying operation of the thruster, and giving initial estimates of thrust and ISP performance. The stand also allows for simplified placement and mounting within the chamber, as well as alignment of the thruster to the Faraday cup input. The test stand was then mounted into the micro propulsion testing chamber, centered in full view in the 6" conflat viewport, and wired up for thruster power and control.

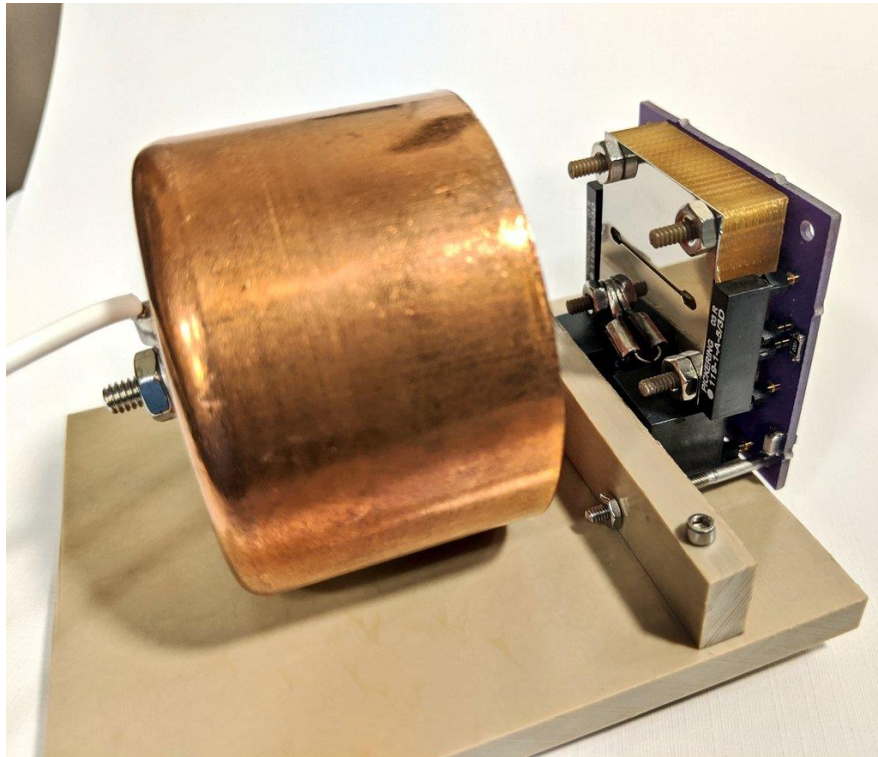


FIGURE 21: AIS-ILIS1 V6 mounted to Faraday cup test stand

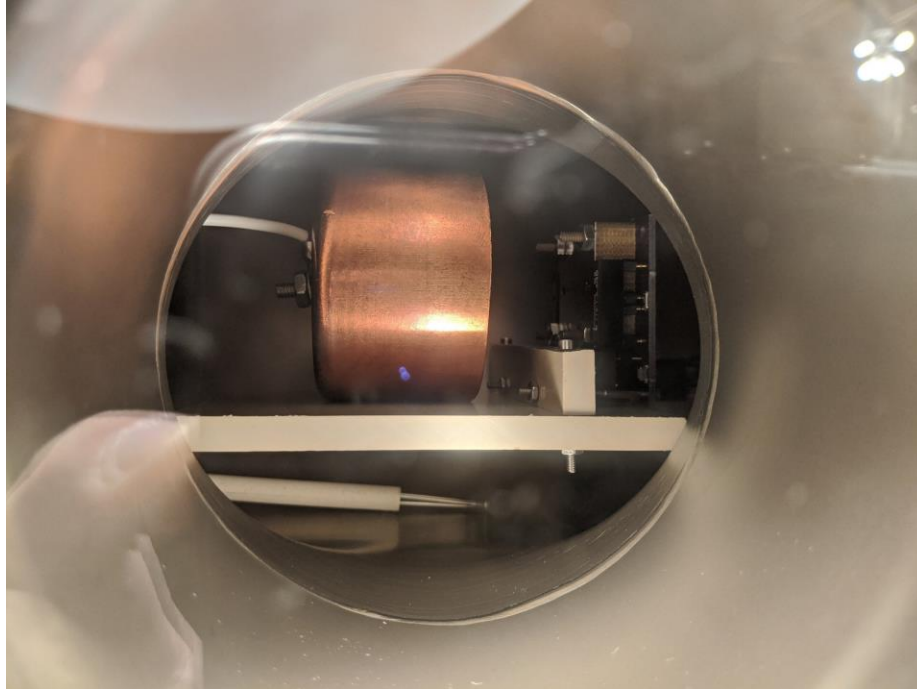


FIGURE 22: ILIS1 and Faraday cup test stand final mounting inside vacuum chamber

VI. TEST PHASE II – IGNITION

The chamber was evacuated to a pressure of 2×10^{-5} Torr before starting up the thruster. In order to better prep the thruster for long duration operation, and slowly bring it up to full power, a new conditioning sequence was adopted, in which the thruster would be operated in monopolar mode, very slowly increasing emitter voltage, before switching polarities, and repeating.

The thruster controls were turned on, and the thruster set to manual monopolar mode operation starting with the +HV. Power was slowly increased, when the thruster emitter flashed briefly, immediately arcing and failed, showing signs of continuous shorting. The test was quickly terminated, and the vacuum system shut down to inspect the thruster.

VII. POST TEST VIDEO ANALYSIS

During the test, video was captured of the thruster during operation. Although the test lasted for only a few seconds before the thruster arced and failed, there was enough video captured to determine key points of fault. It was discovered that during the initial emission flash, the thruster did in fact exhibit multi-site emission along the central region of the emitter. In addition, no arcing or emission was observed at the emitter edges. This was the first time that evidence of multi-site emission along the central length of the ridge was captured for the ILIS1.



FIGURE 23: Captured ion beam emission glow from multi-site emission along the length of the ridge emitter prior to failure (outlined in red.)

VIII. POST TEST THRUSTER INSPECTION

After testing the thruster was removed from the chamber for disassembly and inspection. It was immediately observed that there were several burn marks at various points along the ridge emitter, indicating the areas the thruster shorted at between the emitter and extractor. However, no burning, arcing, or emission was observed at the edges, confirming the new extractor design functioned as expected in reducing field enhancement at the corners, and forcing high field strength along the central region of the ridge.



FIGURE 24: Arcing and fuel deposit on the underside of the extractor

IX. CONCLUSION

The third fueling and ignition test of the AIS-ILIS1 ionic liquid ion source electrospray thruster was completed. Unfortunately, spacing and tolerances were too tight between the emitter and extractor for this iteration, causing rapid shorting and failure of the thruster. Due to lack of proper indexing, as well as the microscope not having enough stage depth to view the assembled thruster, alignment was extremely difficult and had to be done visually as best as possible holding the thruster up to a light and trying to center the ridge with the narrow extractor.

During the recorded test video however, multi-site emission was observed across the length of the ridge emitter, and no damage, emission, or arcing was found at the corners, confirming the extractor behaved as designed. In addition, the arcing intensity was significantly reduced from prior tests, showing that the surge protection resistors greatly inhibited arcing current, and arc energy as a result.

Although successful ignition across the ridge emitter was not achieved, and the thruster failed very rapidly, enough data was collected confirming several of the preliminary changes to the design. Key takeaways of the test include:

- Flaring the ends of the extractor slit can eliminate spurious corner emissions and early turn-on at the ridge emitter corners

- Focusing the field strength along the central region of the emitter and reducing field strength at the edges can allow for multi-site emission to occur
- Surge protection resistors are important for limiting arcing energy and subsequent damage
- 0.5 mm aperture width at 0 mm height between the ridge and extractor plate is too narrow to be aligned visually without precision manufacturing, keying, and microscopic alignment
- Extractors must be inspected for manufacturing discrepancies, and post-processing of the aperture edges may be needed depending on the quality of manufacture

Going forward, there are several major improvements that can be made to increase the chances of success. The extractor aperture must either be wider, and/or the spacing between the emitter and extractor must be increased to prevent immediate arcing or liquid bridging. In addition, proper alignment is critical for such tight tolerances, requiring better manufacturing and assembly procedures. Higher quality extractors should be investigated, and the addition of keying for assembly should be incorporated in future design iterations.